Exploring accelerated expansion in the universe: A study of $f(Q,T)$ gravity with parameterized EoS and cosmological constraints

M. Koussour [ID],[1, *] N. Myrzakulov [ID],[2, †] J. Rayimbaev [ID],[3, 4, 5, ‡] A. Errehymy [ID],[6, §] and Orhan Donmez [ID][7, ¶]

[1]*Department of Physics, University of Hassan II Casablanca, Morocco.*
[2]*L. N. Gumilyov Eurasian National University, Astana 010008, Kazakhstan.*
[3]*New Uzbekistan University, Mustaqillik Ave. 54, Tashkent 100007, Uzbekistan.*
[4]*University of Tashkent for Applied Sciences, Gavhar Str. 1, Tashkent 100149, Uzbekistan.*
[5]*National University of Uzbekistan, Tashkent 100174, Uzbekistan.*
[6]*Astrophysics Research Centre, School of Mathematics, Statistics and Computer Science,*
University of KwaZulu-Natal, Private Bag X54001, Durban 4000, South Africa
[7]*College of Engineering and Technology, American University of the Middle East, Egaila 54200, Kuwait*
(Dated: April 23, 2024)

The study conducted in this research paper utilizes the $f(Q,T)$ gravity, where Q represents non-metricity and T represents the trace of the energy-momentum tensor, to investigate the accelerated expansion of the universe. To complete the study, an effective EoS with one parameter α, is parameterized as $\omega_{eff} = -\frac{3}{\alpha(1+z)^3+3}$. The linear version of $f(Q,T) = -Q + \sigma T$ is also considered, where σ is a constant. By constraining the model with six BAO points, 57 Hubble points, and 1048 Pantheon sample datasets, the parameters α and σ are determined to best match the data. The cosmological parameters and energy conditions for the model are derived and examined. The results show that the model is in good agreement with observations, and can serve as a valuable starting point for analyzing FLRW models in the $f(Q,T)$ theory of gravity.

I. INTRODUCTION

It is thought that the expansion of our universe is accelerating. Dark Energy (DE), a mysterious type of energy with extremely high negative pressure, is thought to be the cause of this. Various cosmological observations have supported the existence of this sort of energy [1–8]. Its precise nature, however, is still an unresolved issue that requires more research. The cosmological constant is the earliest and most straightforward option for DE, but it has two significant theoretical issues, including coincidence and fine-tuning concerns [9]. The coincidence problem arises from the fact that the energy density of DE and matter in the universe are of the same order of magnitude at the present epoch, despite evolving differently over cosmic history. The fine-tuning problem, on the other hand, relates to the extremely small but non-zero value of the cosmological constant required to match observations. The energy density associated with the cosmological constant is many orders of magnitude smaller than what would be expected based on quantum field theory calculations [10]. To solve the DE problem, two methods have been proposed: One involves

studying the dynamics of various DE models, and the other entails modifying the Hilbert–Einstein action of General Relativity (GR), which results in altered theories of gravity. The Equation of State (EoS) parameter $\omega_{DE} = \frac{p_{DE}}{\rho_{DE}}$, where p_{DE} is really the pressure and ρ_{DE} is the energy density of DE, allows the DE models to be separated from the cosmological constant (also known as ΛCDM model). The ΛCDM model is supported by the EoS parameter value of $\omega_0 = -1.084 \pm 0.063$ and $\omega_0 = -1.073^{+0.090}_{-0.089}$ from observational sources, Supernova data and WMAP, respectively [11, 12]. The most well-known DE models are the interactive DE models, such as the Chaplygin gas family, Braneworld, holographic DE (HDE), agegraphic DE models, etc [13–16]. Scalar field models, such as quintessence ($-1 < \omega_{DE} < -\frac{1}{3}$), phantom ($\omega_{DE} < -1$), k-essence, tachyon, and quintom, are also well-known [17–19]. The quintessence and phantom DE theories are also supported by the observed value of the EoS parameter.

The $f(R)$ and $f(R,T)$ theories of gravity, where R and T denote the curvature scalar and the trace of the energy-momentum tensor, respectively, are crucial in explaining the DE models among the different alternative theories. The Refs. [20–22] provide a thorough overview of both modified theories of gravity and DE models. In addition to $f(R)$ and $f(R,T)$ theories, there has been significant research on other geometrically extended theories of gravity that aim to explain the accelerated cosmic expansion. For example, $f(R, L_m)$ grav-

ity, where L_m is the matter Lagrangian density, has been proposed as an alternative to GR [23–26]. Similarly, $f(G)$ gravity, where G is the Gauss-Bonnet invariant [27], and $f(R, G)$ gravity, which combines modifications to the gravitational action involving both R and G [28, 29], have also been proposed as alternative theories of gravity that could explain the accelerated cosmic expansion. All of the aforementioned extensions of GR share the fundamental Riemannian geometry that forms the basis of such classical concepts, especially GR [30]. Due to the inconsistency of these concepts at certain scales, it follows logically that if the fundamental geometry could be replaced with a much more universal geometric framework, we might be able to eliminate some of the contradictions (such as the dark matter (DM) and DE that have dogged these classical concepts over the years. Weyl made such an innovative effort, where the geometric unification of gravity and magnetism was the primary goal [31]. We are aware that the Levi-Civita connection, which is the fundamental method for comparing the lengths of vectors in Riemannian geometry, is compatible with the metric. The mechanism utilized in Weyl's theory has two connections, one of which contains the vector's length information and the other of which determines the vector's direction throughout parallel transport. The electromagnetic potential is physically linked to the length connection. The non-zero covariant divergence of the metric tensor i.e. $\nabla_\gamma g_{\mu\nu} \neq 0$, which is a trait that leads to a additional geometric quantity called the non-metricity Q, is the most remarkable aspect of the theory. There are two different representations of GR that we can find in the literature: the first one has $R \neq 0$, $T = 0$ (here T is the torsion), and $Q = 0$ (curvature representation), while the second one has $R = 0$, $T \neq 0$, and $Q = 0$ (teleparallel representation) [32–34]. Therefore, the non-metricity Q disappears in each of these representations. Geometrically, Q depicts the variation in a vector's length in parallel transport. Now, a non-vanishing non-metricity Q was thought of as the fundamental geometrical variable accountable for all varieties of gravitational interactions in a third equivalent representation of GR. The symmetric teleparallel gravity (STG) is the name given to this theory [35]. In [36, 37], the cosmology of $f(Q)$ gravity and its observational constraints were examined. There have been a number of publications in the STG framework during the past few decades [38–46].

According to the authors of Ref. [47], the non-minimal coupling between the matter Lagrangian L_m and the non-metricity scalar Q allows for an extension of the $f(Q)$ theory of gravity. As would be predicted, the non-minimal coupling between the geometry and matter sectors causes the energy-momentum tensor to not be conserved and causes an additional force to appear in the geodesic equation of motion. Another generalization of the $f(Q)$ theory, known as the $f(Q, T)$ theory, was proposed by Xu et al. [48], where the gravity Lagrangian is essentially an arbitrary function of the non-metricity scalar Q and the trace of the energy-momentum tensor T. The cosmic evolution was investigated while the field equations were being developed. It was discovered that the theory indicated an accelerated expansion of the universe culminating in a de-Sitter type evolution in all situations taken into consideration. In $f(Q, T)$ gravity, the late-time cosmology in the hybrid expansion law [49] and the bouncing scenarios [50] are examined. Also, baryogenesis in $f(Q, T)$ gravity was studied by Bhattacharjee et al. [51].

The work is structured as follows: in Sec. II, the action of $f(Q, T)$ gravity and fundamental field equations are provided. In Sec. III, we discussed the parametrization of the effective EoS parameter and the energy conditions. We have discussed and analyzed our model in $f(Q, T)$ gravity using some observational datasets in Sec. III. In Sec. IV, the findings and conclusions are discussed.

II. $f(Q, T)$ **GRAVITY THEORY**

The action used to determine $f(Q, T)$ gravity is defined as [48],

$$S = \int \sqrt{-g}d^4x \left(\frac{1}{16\pi} f(Q, T) + L_m \right). \tag{1}$$

Here, $f(Q, T)$ is an arbitrary function that correlates the trace of the energy-momentum tensor T to its non-metricity Q. Additionally, L_m stands for the matter Lagrangian, and $g = det(g_{\mu\nu})$. The non-metricity Q is also described as [35],

$$Q \equiv -g^{\mu\nu}(L^\beta{}_{\alpha\mu}L^\alpha{}_{\nu\beta} - L^\beta{}_{\alpha\beta}L^\alpha{}_{\mu\nu}), \tag{2}$$

where $L^\beta{}_{\alpha\gamma}$ is the abbreviation for the disformation tensor,

$$L^\beta{}_{\alpha\gamma} = -\frac{1}{2}g^{\beta\eta}(\nabla_\gamma g_{\alpha\eta} + \nabla_\alpha g_{\eta\gamma} - \nabla_\eta g_{\alpha\gamma}). \tag{3}$$

$$= \frac{1}{2}g^{\beta\eta}\left(Q_{\gamma\alpha\eta} + Q_{\alpha\eta\gamma} - Q_{\eta\alpha\gamma} \right), \tag{4}$$

$$= L^\beta{}_{\gamma\alpha}. \tag{5}$$

The tensor of non-metricity is denoted by,

$$Q_{\gamma\mu\nu} = -\nabla_\gamma g_{\mu\nu} = -\partial_\gamma g_{\mu\nu} + g_{\nu\sigma}\widetilde{\Gamma}^\sigma{}_{\mu\gamma} + g_{\sigma\mu}\widetilde{\Gamma}^\sigma{}_{\nu\gamma}, \tag{6}$$

where $\widetilde{\Gamma}^\sigma{}_{\mu\gamma}$ is the Weyl–Cartan connection [48], and the trace of the non-metricity tensor being provided as,

$$Q_\beta = g^{\mu\nu} Q_{\beta\mu\nu}, \qquad \widetilde{Q}_\beta = g^{\mu\nu} Q_{\mu\beta\nu}. \tag{7}$$

A superpotential or the non-metricity conjugate can also be defined as,

$$P^\beta{}_{\mu\nu} \equiv \frac{1}{4} \Bigg[-Q^\beta{}_{\mu\nu} + 2Q_{(\mu}{}^\beta{}_{\nu)} + Q^\beta g_{\mu\nu} - \widetilde{Q}^\beta g_{\mu\nu}$$

$$-\delta^\beta{}_{(\mu} Q_{\nu)} \Bigg] = -\frac{1}{2} L^\beta{}_{\mu\nu} + \frac{1}{4}\left(Q^\beta - \widetilde{Q}^\beta \right) g_{\mu\nu} - \frac{1}{4}\delta^\beta{}_{(\mu}Q_{\nu)} \tag{8}$$

expressing the scalar of non-metricity as [35],

$$Q = -Q_{\beta\mu\nu} P^{\beta\mu\nu} = -\frac{1}{4}\Big(-Q^{\beta\nu\rho}Q_{\beta\nu\rho} + 2Q^{\beta\nu\rho}Q_{\rho\beta\nu}$$

$$-2Q^\rho \widetilde{Q}_\rho + Q^\rho Q_\rho \Big). \tag{9}$$

As a result, by equating the variation of action in Eq. (1) with regard to the metric tensor to zero i.e. $\delta S = 0$, we obtain the following field equations:

$$-\frac{2}{\sqrt{-g}}\nabla_\beta(f_Q\sqrt{-g}P^\beta{}_{\mu\nu}) - \frac{1}{2}fg_{\mu\nu} + f_T(T_{\mu\nu} + \Theta_{\mu\nu})$$

$$- f_Q(P_{\mu\beta\alpha}Q_\nu{}^{\beta\alpha} - 2Q^{\beta\alpha}{}_\mu P_{\beta\alpha\nu}) = 8\pi T_{\mu\nu}. \tag{10}$$

Here, $f_Q = \dfrac{df}{dQ}$, $f_T = \dfrac{df}{dT}$ and $T_{\mu\nu}$ is the energy-momentum tensor for the fluid of the ideal type, as described by

$$T_{\mu\nu} = -\frac{2}{\sqrt{-g}}\frac{\delta(\sqrt{-g}L_m)}{\delta g^{\mu\nu}} \tag{11}$$

and

$$\Theta_{\mu\nu} = g^{\alpha\beta}\frac{\delta T_{\alpha\beta}}{\delta g^{\mu\nu}}. \tag{12}$$

Moreover, the variation of energy-momentum tensor with respect to the metric tensor is,

$$\frac{\delta g^{\mu\nu} T_{\mu\nu}}{\delta g^{\alpha\beta}} = T_{\alpha\beta} + \Theta_{\alpha\beta}. \tag{13}$$

Now, suppose the universe can be represented by the homogeneous, isotropic, and spatially flat FLRW metric,

$$ds^2 = -dt^2 + a^2(t)\left[dx^2 + dy^2 + dz^2 \right], \tag{14}$$

where $a(t)$ is the scale factor of the universe used to estimate the rate of cosmic expansion at a time t. Further, it is presumed that the known universe matter is made up

of a perfect fluid, for which the energy-momentum tensor, $T^\mu{}_\nu = diag(-\rho, p, p, p)$. Moreover, the non-metricity scalar Q for this type of metric is derived and given as $Q = 6H^2$, where H is the Hubble parameter.

The generalized Friedmann equations are given below by using the metric (14) and the field equation (10),

$$8\pi\rho = \frac{f}{2} - 6FH^2 - \frac{2\widetilde{G}}{1 + \widetilde{G}}(\dot{F}H + F\dot{H}), \tag{15}$$

$$8\pi p = -\frac{f}{2} + 6FH^2 + 2(\dot{F}H + F\dot{H}), \tag{16}$$

where, the dot ($\cdot$) denotes a derivative with respect to time, while the symbols $F = f_Q$, and $8\pi\widetilde{G} = f_T$, respectively, signify differentiation with respect to Q, and T.

Using the two Eqs. (15) and (16) mentioned above , we can construct the equations similar to the form of standard GR,

$$3H^2 = 8\pi\rho_{eff} = \frac{f}{4F} - \frac{4\pi}{F}\left[(1 + \widetilde{G})\rho + \widetilde{G}p \right], \tag{17}$$

and

$$2\dot{H} + 3H^2 = -8\pi p_{eff} = \frac{f}{4F} - \frac{2\dot{F}H}{F} +$$

$$\frac{4\pi}{F}\left[(1 + \widetilde{G})\rho + (2 + \widetilde{G})p \right], \tag{18}$$

where the terms ρ_{eff}, and p_{eff} refer to the effective pressure and density, respectively.

III. PARAMETRIZATION OF THE EFFECTIVE EOS PARAMETER

The system of field equations, discussed as Eqs. (15) and (16), contains only two independent equations with four unknowns: $f(Q, T), \rho, p$, and H. Therefore, two additional constraint equations are required to fully solve the system and study the temporal evolution of the energy density and pressure. The use of these equations is supported by several justifications in the literature, such as the model-independent way approach to studying DE models [52, 53]. This approach typically involves a parametrization of kinematic variables, such as the Hubble parameter, deceleration parameter, EoS parameter, and jerk parameter, and provides the necessary supplementary equation. The primary advantage of this method is that it allows for the examination of cosmological models using observational data. The relationship between the scale factor $a(t)$ and the redshift z is known to be represented by $\frac{a_0}{a} = 1 + z$, where a_0 is the present value of scale factor ($a_0 = a(0) = 1$).

From the relationship mentioned above, we may conclude $\frac{d}{dt} = \frac{dz}{dt}\frac{d}{dz} = -(1+z)H(z)\frac{d}{dz}$. Thus, the Hubble parameter can be expressed mathematically as,

$$\dot{H} = -(1+z)H(z)\frac{dH}{dz}. \tag{19}$$

In the context of this investigation, we will employ the following functional expression: $f(Q,T) = \chi Q + \sigma T$, where χ and σ are model parameters. This model was first proposed by Xu et al. [48] to describe an exponentially expanding universe, where the energy density ρ scales as $\exp(-H_0 t)$. It has since been constrained by observational data related to the Hubble parameter, as detailed in [54]. Loo et al. [55] utilized this model to study Bianchi type-I cosmology, incorporating observational datasets such as Type Ia supernovae and the Hubble parameter. In addition, [56] explored wormhole solutions within this model, considering various EoS relations. Hence, we have $F = f_Q = \chi$ and $8\pi\widetilde{G} = f_T = \sigma$. In this scenario, setting $\chi = -1$ and $\sigma = 0$ leads to the well-motivated case of General Relativity (GR). In our study, we choose $\chi = -1$ to facilitate the derivation of solutions corresponding to GR. In addition, it's worth noting that these solutions remain independent of the parameter χ. Next, the Friedmann equations (15) and (16) for this particular $f(Q,T)$ model give the following expressions for the energy density and pressure in terms of redshift,

$$\rho = \frac{3H^2 + \dot{H}}{8\pi + 2\sigma} - \frac{\dot{H}}{8\pi + \sigma}, \tag{20}$$

and

$$p = -\frac{3H^2 + \dot{H}}{8\pi + 2\sigma} - \frac{\dot{H}}{8\pi + \sigma}. \tag{21}$$

The EoS parameter $\omega = \frac{p}{\rho}$ was determined as the effective or total EoS parameter,

$$\omega = \frac{3H^2(8\pi + \sigma) + \dot{H}(16\pi + 3\sigma)}{\sigma\dot{H} - 3H^2(8\pi + \sigma)}. \tag{22}$$

Now, a single assumption is necessary to solve the system of equations, specifically Eqs. (15) and (16).

Recent studies have investigated various parametrizations of the EoS. The Chevallier-Polarski-Linder (CPL) parametrization, which is based on a simple Taylor expansion of the EoS with respect to the scale factor, is the most widely used parametrization. It is represented by $\omega = \omega_0 + \omega_1\frac{z}{1+z}$ [57, 58]. Other popular parametrizations include the Jassal-Bagla-Padmanabhan (JBP) parametrization, which permits the transition from a DE-dominated universe to a matter-dominated universe, and is expressed as $\omega = \omega_0 + \omega_1\frac{z}{(1+z)^2}$ [59], and the Ma-Zhang (MZ) parametrization, which is based on a logarithmic and oscillating form of the EoS. Specifically, the MZ parametrization has two forms: $\omega = \omega_0 + \omega_1(\frac{\ln(2+z)}{1+z} - \ln 2)$ and $\omega = \omega_0 + \omega_1(\frac{\sin(1+z)}{1+z} - \sin(2))$ [60]. The paper under consideration examines the following parametric form of the effective (or total) EoS as a function of redshift z [61],

$$\omega_{eff} = -\frac{3}{\alpha(1+z)^3 + 3}, \tag{23}$$

where α is a constant parameter. This specific form of ω_{eff} is motivated by many studies in the literature that utilize single-parameter EoS, which are commonly used in cosmology and astrophysics for their simplicity and effectiveness in capturing key aspects of the system [61–63]. These models have proven successful in describing a variety of phenomena, highlighting their importance in theoretical and observational studies of the universe. Also, we chose this form because it shows interesting behavior during the early stages of the universe's evolution. At large values of z, ω_{eff} is close to zero, resembling the EoS of non-pressurized fluid like DM. As the universe evolves, ω_{eff} becomes increasingly negative, indicating negative pressure. Setting α to zero results in ω_{eff} being -1, equivalent to a cosmological constant. For α less than -1, the model shows phantom behavior, with ω_{eff} dropping below -1. Unlike traditional DE models that are limited to the early stages and later dominate over DM, this model behaves like pressureless DM in its early stages, when ω_{eff} approaches zero [61].

The differential equation for $H(z)$ is given by Eqs. (19) and (22) with the assumed ansatz of ω_{eff} as shown in Eq. (23),

$$\frac{-3(8\pi + \sigma)H^2 + (16\pi + 3\sigma)(1+z)H(z)\frac{dH}{dz}}{\sigma(1+z)H(z)\frac{dH}{dz} + 3(8\pi + \sigma)H^2} = -\frac{3}{\alpha(1+z)^3 + 3} \tag{24}$$

Thus, the solution derived for the Hubble parameter $H(z)$ as a function of redshift z is,

$$H(z) = H_0\left[\frac{12\sigma + 3\alpha\sigma(z+1)^3 + 16\pi\alpha(z+1)^3 + 48\pi}{3(\alpha+4)\sigma + 16\pi(\alpha+3)}\right]^{\frac{\sigma+8\pi}{3\sigma+16\pi}}, \tag{25}$$

where H_0 represents the present value (i.e. at $z = 0$) of the Hubble parameter. Specifically, in the case where $\sigma = 0$, the solution simplifies to $f(Q,T) = -Q$. This directly corresponds to the Λ CDM model. Consequently, the Hubble parameter equation $H(z)$ can be expressed as

$$H(z) = H_0 \left[\Omega_{m0} (1+z)^3 + \Omega_\Lambda \right]^{\frac{1}{2}} \qquad (26)$$

where $\Omega_{m0} = \frac{\alpha}{3+\alpha}$ and $\Omega_\Lambda = (1 - \Omega_{m0}) = \frac{3}{3+\alpha}$ denote the present density parameters for matter and the cosmological constant, respectively. Therefore, the model parameter σ serves as a reliable indicator of the current model's deviation from the ΛCDM model, arising from the inclusion of the trace of the energy-momentum tensor terms.

As a dimensionless representation of the second order time derivative of the scale factor of the universe, the deceleration parameter is defined as, $q = -\frac{\ddot{a}}{aH^2}$. Moreover, it can be expressed using the Hubble parameter and its derivative in terms of the cosmological redshift as [48],

$$q(z) = -1 + (1+z) \frac{1}{H(z)} \frac{dH(z)}{dz}. \qquad (27)$$

The deceleration parameter $q(z)$ establishes the rate of expansion of the universe. The value of $q(z)$ affects the expansion of the universe. In other words, the universe exhibits acceleration if $q(z) < 0$ or deceleration

if $q(z) > 0$ whereas $q(z) = 0$ denotes expansion at a constant rate. For the present parametrization of the effective EoS, the expression of the deceleration parameter obtained by including Eq. (25) into Eq. (27) as,

$$q(z) = -1 + \frac{3\alpha(\sigma + 8\pi)(z+1)^3}{3\sigma\left(\alpha(z+1)^3 + 4\right) + 16\pi\left(\alpha(z+1)^3 + 3\right)}. \qquad (28)$$

In addition, the third-order time derivative of the scale factor of the universe is represented without dimensions by the jerk parameter j, which is defined as, $j = \frac{\dddot{a}}{aH^3}$. The deceleration parameter and its derivative with respect to the cosmological redshift can also be used to express the jerk parameter as,

$$j(z) = (1+z) \frac{dq(z)}{dz} + q(z)(1 + 2q(z)). \qquad (29)$$

According to popular belief, a cosmic jerk caused the transition from the decelerating state to the accelerating state of the universe. For various models with a positive value for the jerk parameter and a negative value for the deceleration parameter, the universe transitions in this way [64, 65]. For instance, the ΛCDM models have a fixed jerk of $j(z) = 1$. Moreover, the expression for the current model is

$$j(z) = \frac{8\left(9\sigma^2\left(\alpha(z+1)^3 + 2\right) + 3\pi\sigma\left(\alpha(z+1)^3\left(\alpha(z+1)^3 + 28\right) + 48\right) + 32\pi^2\left(\alpha(z+1)^3 + 3\right)^2\right)}{\left(3\sigma\left(\alpha(z+1)^3 + 4\right) + 16\pi\left(\alpha(z+1)^3 + 3\right)\right)^2}. \qquad (30)$$

We are aware that certain physical parameters, including the EoS parameter, the jerk parameter and the deceleration parameter, are crucial in the study of the universe. An important new study in contemporary cosmology is on the energy conditions derived from the

Raychaudhuri equation [66]. Further, we have investigated the evolution of the most fundamental energy conditions used in GR [67]. These conditions, place further constraints on the validity of the proposed cosmological model, which are specified as follows:

$$\text{WEC}: \rho = \frac{6H_0^2\left(\alpha(z+1)^3 + 3\right)\left(\frac{3\sigma\left(\alpha(z+1)^3+4\right)+16\pi\left(\alpha(z+1)^3+3\right)}{3(\alpha+4)\sigma+16\pi(\alpha+3)}\right)^{-\frac{\sigma}{3\sigma+16\pi}}}{3(\alpha+4)\sigma + 16\pi(\alpha+3)} \geq 0 \qquad (31)$$

$$\text{NEC}: \rho + p = \frac{6\alpha H_0^2(z+1)^3\left(\frac{3\sigma\left(\alpha(z+1)^3+4\right)+16\pi\left(\alpha(z+1)^3+3\right)}{3(\alpha+4)\sigma+16\pi(\alpha+3)}\right)^{-\frac{\sigma}{3\sigma+16\pi}}}{3(\alpha+4)\sigma + 16\pi(\alpha+3)} \geq 0 \qquad (32)$$

$$\text{DEC} : \rho - p = \frac{6H_0^2 \left(\alpha(z+1)^3 + 6\right) \left(\frac{3\sigma\left(\alpha(z+1)^3+4\right)+16\pi\left(\alpha(z+1)^3+3\right)}{3(\alpha+4)\sigma+16\pi(\alpha+3)}\right)^{-\frac{\sigma}{3\sigma+16\pi}}}{3(\alpha+4)\sigma+16\pi(\alpha+3)} \geq 0 \tag{33}$$

$$\text{SEC} : \rho + 3p = \frac{6H_0^2 \left(\alpha(z+1)^3 - 6\right) \left(\frac{3\sigma\left(\alpha(z+1)^3+4\right)+16\pi\left(\alpha(z+1)^3+3\right)}{3(\alpha+4)\sigma+16\pi(\alpha+3)}\right)^{-\frac{\sigma}{3\sigma+16\pi}}}{3(\alpha+4)\sigma+16\pi(\alpha+3)} \geq 0 \tag{34}$$

where, WEC, NEC, DEC, and SEC represent weak energy conditions, null energy conditions, dominant energy conditions, and strong energy conditions, respectively. The null energy condition violation leads to the remaining energy condition violation, which symbolizes the universe expanding as its energy density is being depleted. Also, the strong energy condition violation symbolizes the acceleration of the universe [68].

To study the evolution of the cosmological parameters of the model, we will need to constrain the model's parameters i.e. α and σ using some recent observational data.

IV.   OBSERVATIONAL CONSTRAINTS FROM BAO, HUBBLE, AND SNE DATASETS

The estimate of the parameter values from the observational data is a critical element of the parametrization method. The model has two parameters: the parameter given by the ω_{eff} equation i.e. α and the coupling constant of model σ. In this part, we examine the observational features of our present parametrization of the effective EoS. To determine the model parameters α and σ ranges that best suit the data, we analyze six points of the baryonic acoustic oscillations datasets (BAO), 57 points of the Hubble datasets, and 1048 points from the Pantheon supernovae Ia sample datasets (SNe). We use the MCMC (Markov Chain Monte Carlo) approach in the emcee python library [69] together with the standard Bayesian method and likelihood function to constrain the model parameters.

A.   BAO datasets

The BAO distance datasets consists of BAO measurements at six different redshifts for the 6dFGS, SDSS, and

WiggleZ surveys. The comoving sound horizon r_s at the photon decoupling epoch z_*, which is defined by the following relation, governs the characteristic scale of BAO:

$$r_s(z_*) = \frac{c}{\sqrt{3}} \int_0^{\frac{1}{1+z_*}} \frac{da}{a^2 H(a)\sqrt{1 + (3\Omega_{b0}/4\Omega_{\gamma0})a}}. \tag{35}$$

where $\Omega_{\gamma0}$ represents the photon density parameter at the moment and Ω_{b0} represents the baryon density parameter at the moment.

In this work, to measure BAO, the following relationships are used,

$$\triangle\theta = \frac{r_s}{d_A(z)}, \, d_A(z) = \int_0^z \frac{dz'}{H(z')}, \, \triangle z = H(z)r_s. \tag{36}$$

Here, $\triangle z$ is the observed redshift separation of the BAO measurements in the two-point correlation function of the galaxy distribution on the sky along the line of sight, $\triangle\theta$ denotes the observed angular separation, and d_A is the angular diameter distance. Six-point BAO datasets for $d_A(z_*)/D_V(z_{BAO})$ are obtained from the Refs. [70–75], where $d_A(z)$ denotes the co-moving angular diameter distance together with the dilation scale $D_V(z) = \left[d_A(z)^2 z/H(z)\right]^{1/3}$. Also, the Planck measurements show that the redshift value for the photon decoupling epoch is $z_* \approx 1091$. The chi-square function for the BAO sets of data is defined as [75],

$$\chi^2_{BAO} = X^T C^{-1} X, \tag{37}$$

where

$$X = \begin{pmatrix} \frac{d_A(z_\star)}{D_V(0.106)} - 30.95 \\ \frac{d_A(z_\star)}{D_V(0.2)} - 17.55 \\ \frac{d_A(z_\star)}{D_V(0.35)} - 10.11 \\ \frac{d_A(z_\star)}{D_V(0.44)} - 8.44 \\ \frac{d_A(z_\star)}{D_V(0.6)} - 6.69 \\ \frac{d_A(z_\star)}{D_V(0.73)} - 5.45 \end{pmatrix},$$

and,

$$C^{-1} = \begin{pmatrix} 0.48435 & -0.101383 & -0.164945 & -0.0305703 & -0.097874 & -0.106738 \\ -0.101383 & 3.2882 & -2.45497 & -0.0787898 & -0.252254 & -0.2751 \\ -0.164945 & -2.454987 & 9.55916 & -0.128187 & -0.410404 & -0.447574 \\ -0.0305703 & -0.0787898 & -0.128187 & 2.78728 & -2.75632 & 1.16437 \\ -0.097874 & -0.252254 & -0.410404 & -2.75632 & 14.9245 & -7.32441 \\ -0.106738 & -0.2751 & -0.447574 & 1.16437 & -7.32441 & 14.5022 \end{pmatrix}.$$

is the inverse of the covariance matrix [75].

$\alpha = 1.32^{+0.32}_{-0.29}$

$\sigma = 0.049^{+0.048}_{-0.046}$
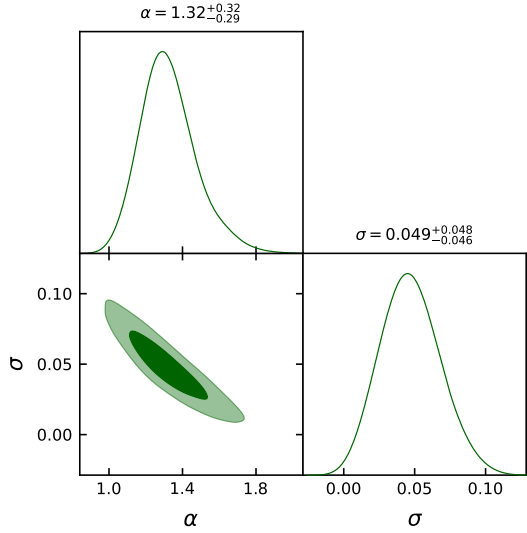
FIG. 1. The $1-\sigma$ and $2-\sigma$ likelihood contours are depicted in this figure, which represents the model parameter space constrained by the BAO datasets

$\alpha = 1.187^{+0.080}_{-0.075}$

$\sigma = 0.048^{+0.048}_{-0.046}$
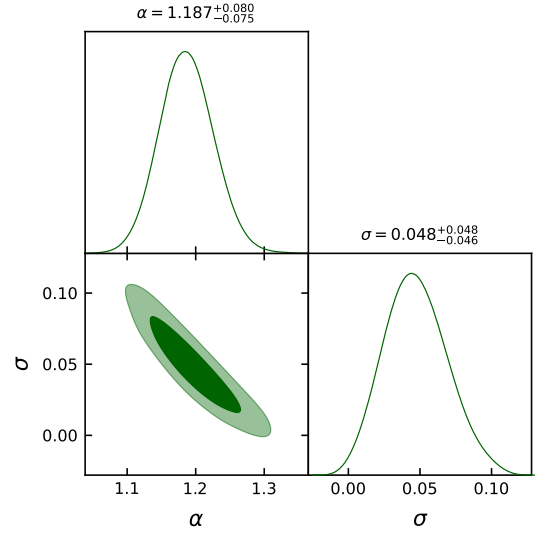
FIG. 2. The $1-\sigma$ and $2-\sigma$ likelihood contours are depicted in this figure, which represents the model parameter space constrained by the BAO+Hubble+SNe datasets.

By minimizing the chi-square function for the BAO, we were able to determine the parameter α and σ ranges for the effective EoS model that best suited the data. Fig. 1 presents the $1-\sigma$ and $2-\sigma$ likelihood contours for the model parameters α and σ using the BAO datasets. The best-fit values that correspond to observations are $\alpha = 1.32^{+0.32}_{-0.29}$, and $\sigma = 0.049^{+0.049}_{-0.046}$.

B. Hubble datasets

Here, the Hubble parameter $H(z)$ has been measured by several teams. By measuring the differential of cosmological redshift z with regard to cosmic time t, it is possible to estimate the value of $H(z)$ as $H(z) = -dz/[dt(1+z)]$. The model-independent value of the Hubble parameter may be determined by measuring the quantity dt since dz is obtained from a spectroscopic survey. We used an updated dataset of 57 Hubble measurements in the $0.07 \leq z \leq 2.41$ range of redshift [76]. The differential age approach and line of sight BAO are two generally accepted methods for determining the values of $H(z)$ at a particular redshift. Further, we have considered $H_0 = 69 \ km/s/Mpc$ in our research [12]. To calculate the mean values of the model parameters α and σ, the chi-square function is defined as,

$$\chi^2_{Hubble}(\alpha, \sigma) = \sum_{i=1}^{57} \frac{[H_{th}(\alpha, \sigma, z_i) - H_{obs}(z_i)]^2}{\sigma^2_{H(z_i)}}, \quad (38)$$

where, H_{obs} is the observed value of the Hubble parameter, H_{th} is the predicted value of the Hubble parameter, and $\sigma_{H(z_i)}$ is the standard error in the observed value of H.

C. SNe datasets

The most popular data sample for studying the late-time evolution of the universe is data from SNe observations. 1048 type Ia supernovae with redshifts z between 0.01 and 2.3 make up the Pantheon samples, which were assembled by Scolnic et al [77]. It includes data from the PanSTARSS1 Medium Deep Survey, SDSS, SNLS, and several low-z and HST samples. The difference between the apparent magnitude (m_B) and absolute magnitude (M_B) of the B band of the measured spectrum is the distance modulus of type Ia SNe. It's described as,

$$\mu(z) = 5log_{10}d_L(z) + \mu_0, \quad (39)$$

where the luminosity distance, or $d_L(z)$, is defined in a spatially flat FLRW universe as,

$$d_L(z) = (1+z) \int_0^z \frac{cdz'}{H(z')}, \quad (40)$$

and

$$\mu_0 = 5log(1/H_0 Mpc) + 25, \quad (41)$$

where c represents the speed of light.

The theoretical distance modulus is correlated with the χ^2_{SNe} function for SNe as,

$$\chi^2_{SNe}(\alpha, \sigma) = \sum_{i=1}^{1048} \frac{[\mu_{obs}(z_i) - \mu_{th}(\alpha, \sigma, z_i)]^2}{\sigma^2(z_i)}, \quad (42)$$

where μ_{obs} is the observed value, μ_{th} is the theoretical value of the distance modulus, and $\sigma^2(z_i)$ is really the standard error of the observed value.

D. BAO+Hubble+SNe datasets

In addition, we use the BAO, Hubble and SNe datasets to obtain joint constraints for the parameters α and σ using the total likelihood function. From this point forward, the appropriate probability and Chi-square functions are provided by,

$$\mathcal{L}_{tot} = \mathcal{L}_{BAO} \times \mathcal{L}_{Hubble} \times \mathcal{L}_{SNe}, \quad (43)$$

and

$$\chi^2_{tot} = \chi^2_{BAO} + \chi^2_{Hubble} + \chi^2_{SNe}. \quad (44)$$

Fig. 2 depicts the $1 - \sigma$ and $2 - \sigma$ likelihood contours for the model parameters α and σ using the BAO+Hubble+SNe datasets. The best-fit values that correspond to observations are $\alpha = 1.187^{+0.080}_{-0.075}$, and $\sigma = 0.048^{+0.048}_{-0.046}$.

Fig. 3 compared our model with the well-known ΛCDM cosmology model while taking into account the value matter density parameter $\Omega_{m_0} = 0.315$ [12]. The Hubble dataset findings, which total 57 data points and their associated error, are also shown in the figure, allowing for an easy comparison of the two models.

A comparison between our $f(Q,T)$ model and the well-known ΛCDM model in cosmology is shown in Fig. 4. The Pantheon experimental findings, 1048 data points, and their error are also shown in the graphic, allowing for a direct comparison between the two models
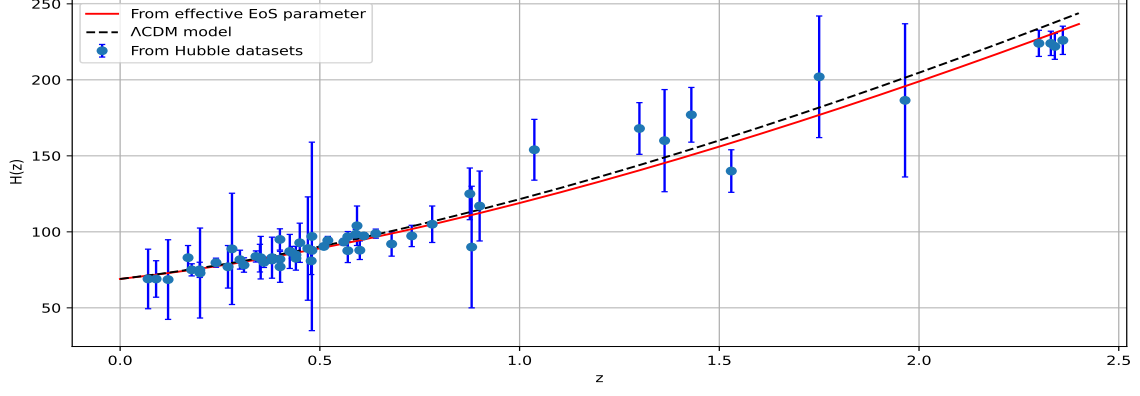
FIG. 3. The graph illustrates a satisfactory correspondence between our $f(Q,T)$ theory and the 57 data points from the Hubble datasets, as depicted by the red curve (in units of $km/s/Mpc$), in comparison to the black dashed line representing ΛCDM, in a plot of $H(z)$ against the redshift z.
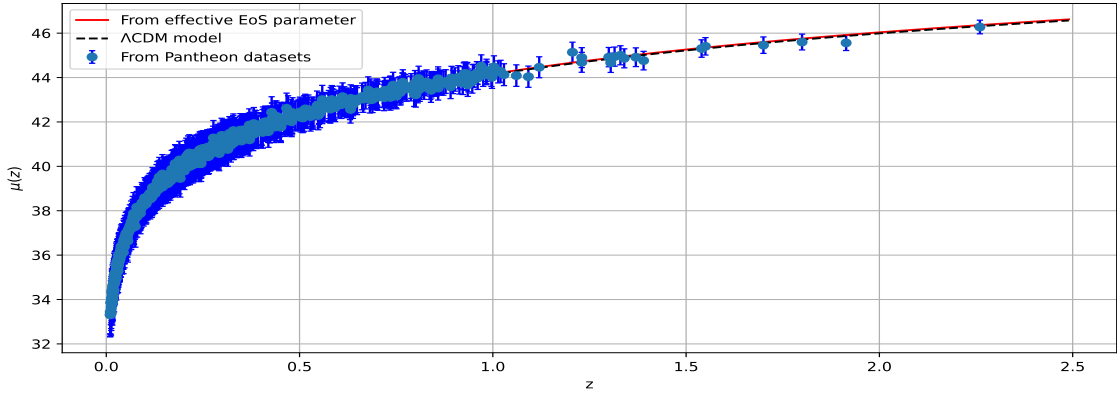

FIG. 4. The graph illustrates a satisfactory correspondence between our $f(Q,T)$ theory and the 1048 points from the Pantheon datasets, as depicted by the red curve, in comparison to the black dashed line representing ΛCDM, in a plot of $\mu(z)$ against the redshift z.

V. DISCUSSION AND CONCLUSION

The parametrization approach has been extensively examined in the literature as a method to address various cosmological challenges. These challenges include the initial singularity problem, the issue of all-time decelerating expansion, the horizon problem, Hubble tension, and more [52, 53]. In our investigation, we introduce a parametric representation for the effective EoS parameter ω_{eff}, as a fundamental aspect of constructing the model within the framework of $f(Q,T)$ gravity theory. This theoretical framework is based on the interplay between the energy-momentum trace T and the non-

metricity scalar Q. The use of a parametric form for ω_{eff} allows for a more flexible and nuanced exploration of the dynamic relationship between these key variables, providing a comprehensive understanding of their interdependence within the context of $f(Q,T)$ gravity theory.

We specifically examine the functional form $f(Q,T) = -Q + \sigma T$, where σ is a free parameter. To solve the field equations for $H(z)$, we employ a parametric form of the ωeff parameter as a function of redshift z. Furthermore, by utilizing BAO datasets and combined BAO+Hubble+SNe datasets, we determine the best-fit values of the model parameters. The results
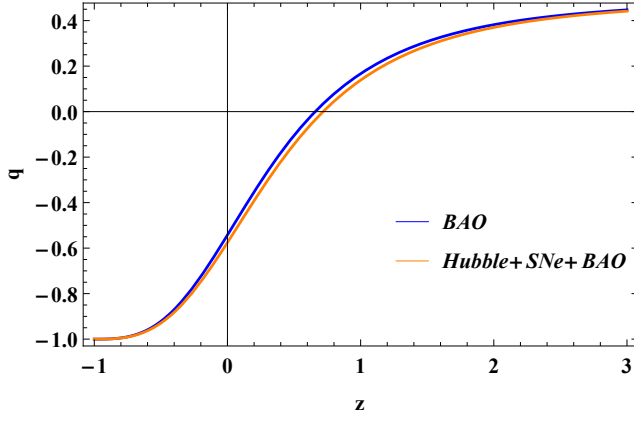
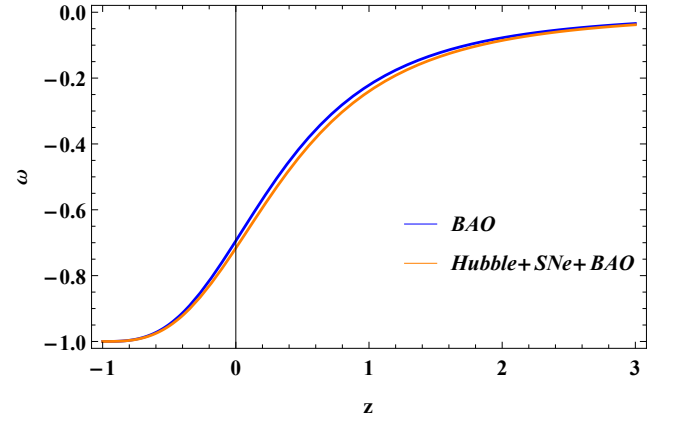FIG. 5. The graph above shows the relationship between the deceleration parameter (q) and redshift (z).

FIG. 8. The graph above shows the relationship between the effective EoS parameter (ω) and redshift (z).
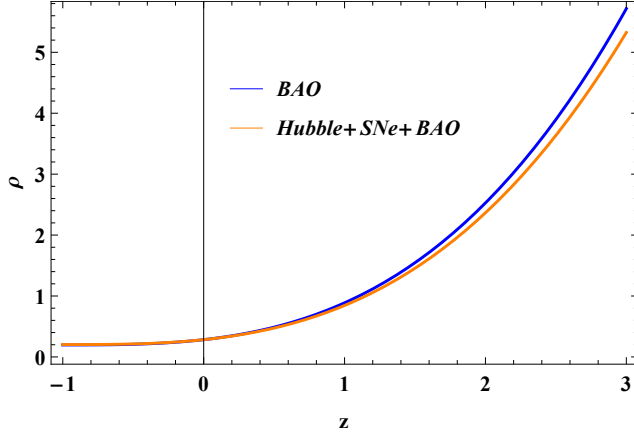

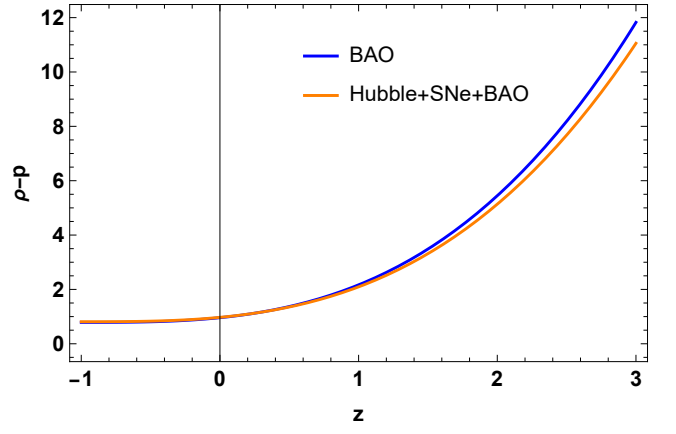FIG. 6. The graph above shows the relationship between the energy density (ρ) and redshift (z).

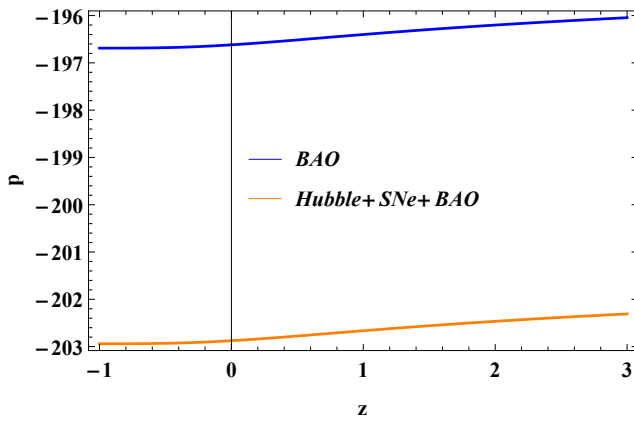FIG. 9. The graph above shows the relationship between the DEC condition and redshift (z).

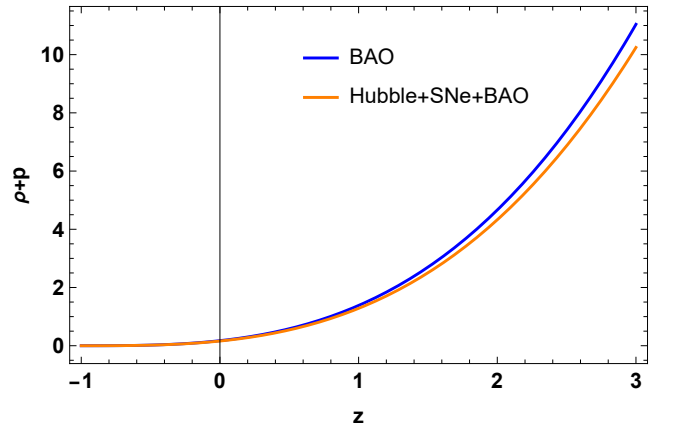FIG. 7. The graph above shows the relationship between the pressure (p) and redshift (z).

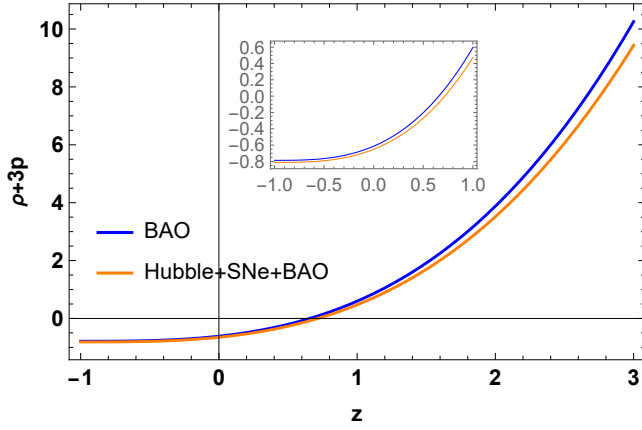FIG. 10. The graph above shows the relationship between the NEC condition and redshift (z).

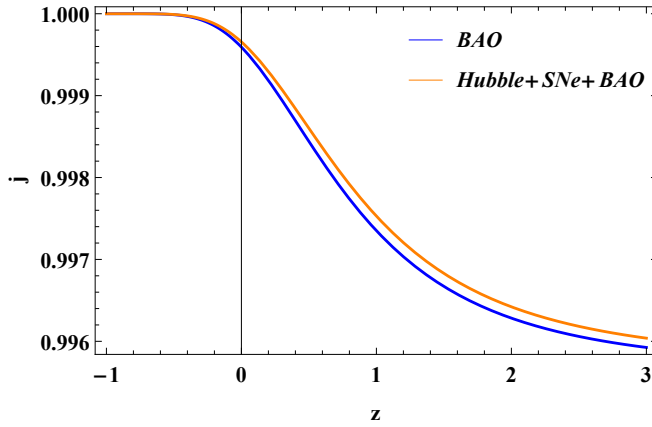FIG. 11. The graph above shows the relationship between the SEC condition and redshift (z).

FIG. 12. The graph above shows the relationship between the jerk parameter (j) and redshift (z).

of the best fit are $\alpha = 1.32^{+0.32}_{-0.29}$, and $\sigma = 0.049^{+0.049}_{-0.046}$ for the BAO datasets and $\alpha = 1.187^{+0.080}_{-0.075}$, and $\sigma = 0.048^{+0.048}_{-0.046}$ for the BAO+Hubble+SNe datasets. In addition, we investigate the behavior of the deceleration parameter, energy density, pressure, effective EoS parameter, and jerk parameter for the constrained values of the model parameters.

In any cosmological model, the deceleration parameter q is a crucial parameter used to characterize the periods of decelerated expansion ($q > 0$) and accelerated expansion ($q < 0$) of the universe. As shown in Eq. (28), it is evident that q approaches -1 as the redshift z approaches -1. The relationship between the deceleration parameter q and the redshift z is illustrated in Fig. 5. To further investigate the nature of the cosmological parameters, we have incorporated the values of the pair (α, σ) obtained from observational data into all our analyses and graphs. It is observed that q

exhibits a transition from early positive values to current negative ones. In this way, the constructed model of the universe develops from an early decelerated period to the present accelerated period. With the observational data, this characteristic is in strong accord. According to the values of the model parameters constrained by BAO, and the combined BAO+Hubble+SNe datasets, the transition redshift are $z_{tr} = 0.6589$ and $z_{tr} = 0.7259$, respectively [78, 79]. Furthermore, the current value of the deceleration parameter is $q_0 = -0.534$ for the BAO datasets and $q_0 = -0.581$ for the combined BAO+Hubble+SNe datasets [80, 81].

The evolution of energy density and pressure, respectively, versus redshift z is depicted in Figs. 6, and 7. It has been shown that the energy density increases positively with redshift z. In addition, from the early era to the present, pressure p has negative values. The current acceleration of the universe may be caused by the negative cosmic pressure. We also examined the behavior of the effective EoS parameter, which is depicted in Fig. 8. The relationship between the previous energy density and pressure is established by the EoS parameter as a whole i.e. $\omega = \frac{p}{\rho}$. The matter phase at $\omega = 0$ is one of the typical phases that may be identified using the EoS parameter. The radiation-dominated phase is then shown by $\omega = \frac{1}{3}$, while $\omega = -1$ represents the ΛCDM model. In addition, the recently discussed accelerating period of the universe, which contains the quintessence ($-1 < \omega < -\frac{1}{3}$) and phantom era ($\omega < -1$), is shown when $\omega < -\frac{1}{3}$. According to the constrained values of α and σ, the effective EoS parameter in Fig. 8 exhibits behavior like quintessence. Also, the value of effective EoS parameter at $z = 0$ is $\omega_0 = -0.7106$ for the BAO datasets and $\omega_0 = -0.7268$ for the combined BAO+Hubble+SNe datasets, which is a definite indication of an accelerating phase [82–84].

The primary objective of energy conditions in cosmology is to assess the expansion behavior of the universe. These conditions serve as crucial indicators of the energy-momentum content of the universe and its impact on cosmic dynamics. Specifically, the violation of the NEC ($\rho + p \geq 0$) implies a violation of the weak ($\rho \geq 0$), dominant ($\rho - p \geq 0$), and strong energy conditions ($\rho + 3p \geq 0$). This violation indicates a decrease in energy density as the universe expands, reflecting the phenomenon of energy dissipation or dilution over cosmic time. Moreover, the violation of the SEC ($\rho + 3p \geq 0$) is particularly significant as it signifies the acceleration of the universe. In our analysis of the energy conditions for the physical model, as shown in Figs. 9-11, we have observed a consistent fulfillment of the WEC ($\rho \geq 0$), NEC ($\rho + p \geq 0$), and DEC ($\rho - p \geq 0$)

throughout the cosmic evolution. These conditions play a crucial role in characterizing the energy-momentum content of the universe and are indicative of its stability and behavior. Notably, the SEC ($\rho + 3p \geq 0$) is found to be violated at late cosmic times, suggesting the presence of exotic forms of energy or modifications to the gravitational theory in these regimes. This violation opens up intriguing possibilities for understanding the nature of DE and the dynamics of the universe at large scales. The relationship between the jerk parameter j and the redshift z is seen in Fig. 12. The graphic shows that throughout cosmic history, $j(z)$ has remained positive. According to Sahni et al. [65], the jerk parameter for the ΛCDM model has a value of $j(z) = 1$. According to Eq. (III), $j(z) \neq 1$ at currently, meaning that the model is currently deviating from ΛCDM. The resultant model, however, behaves in the future as a standard ΛCDM, i.e. $j(z) \to 1$ as $z \to -1$. With current observational data, the results of the model are in strong agreement. The established model is regarded as a helpful reference point for the analysis of FLRW models that include a parametric form of the effective EoS parameter in the $f(Q, T)$ theory of gravity.

[1] A.G. Riess et al., *Astron. J.* **116**, 1009 (1998).
[2] S. Perlmutter et al., *Astrophys. J.* **517**, 565 (1999).
[3] T. Koivisto, D.F. Mota, *Phys. Rev. D* **73**, 083502 (2006).
[4] S.F. Daniel, *Phys. Rev. D* **77**, 103513 (2008).
[5] D.J. Eisenstein et al., *Astrophys. J.* **633**, 560 (2005).
[6] W.J. Percival at el., *Mon. Not. R. Astron. Soc.* **401**, 2148 (2010).
[7] R.R. Caldwell, M. Doran, *Phys. Rev. D* **69**, 103517 (2004).
[8] Z.Y. Huang et al., *J. Cosm. Astrop. Phys.* **0605**, 013 (2006).
[9] S. Weinberg, *Rev. Mod. Phys.* **61**, 1 (1989).
[10] P.J. Steinhardt et al., *Phys. Rev. Lett.*, **59**, 123504 (1999).
[11] G. Hinshaw et al., *Astrophys. J. Suppl.* **208**, 19 (2013).
[12] N. Aghanim et al., *Astron. Astrophys.* **641**, A6 (2020).
[13] A.Y. Kamenshchik et al., *Phys. Lett. B* **511**, 265 (2001).
[14] V. Sahni and Y. Shtanov, *J. Cosmol. Astropart. Phys.* **11**, 014 (2003).
[15] M. Li, *Phys. Lett. B* **603**, 1 (2004).
[16] R. G. Cai, *Phys. Lett. B* **657**, 228 (2007).
[17] T. Padmanabhan, *Phys. Rev. D* **66**, 02131 (2002).
[18] R. R. Caldwell, *Phys. Lett. B* **545**, 23 (2002).
[19] S. Nojiri and S. D. Odintsov, *Phys. Lett. B* **562**, 147 (2003).
[20] E. J. Copeland et al., *Int. J. Mod. Phys. D* **15**, 1753 (2006).
[21] T. Harko et al., *Phys. Rev. D* **84**, 024020 (2011).
[22] S. Nojiri et al., *Phys. Rep.* **692**, 1 (2017).
[23] T. Harko and F. S. N. Lobo, *Eur. Phys. J. C* **70**, 373-379 (2010).
[24] T. Harko, *Phys. Rev. D* **81**, 084050 (2010).
[25] T. Harko, *Phys. Rev. D* **81**, 044021 (2010).
[26] V. Faraoni, *Phys. Rev. D* **76**, 127501 (2007).
[27] A. De Felice and S. Tsujikawa, *Phys. Lett. B* **675**, 1-8 (2009).
[28] M. De Laurentis, M. Paolella, S. Capozziello, *Phys. Rev. D*, **91**, 083531 (2015).
[29] A. de la Cruz-Dombriz, D. S-Gomez, *Class. Quantum Grav.*, **29** 245014 (2012).
[30] B. Riemann, Habilitationsschrift, 1854, *Abh. Koniglichen Ges. Wiss. Gott.* **13**, 1 (1867).
[31] H. Weyl, *Sitz. Preuss. Akad. Wiss.* **465**, 1 (1918).

[32] C. Moller, *Mat. Fys. Skr. Dan. Vid. Selsk.* **1**, 10 (1961).
[33] C. Pellegrini and J. Plebanski, *Mat. Fys. Skr. Dan. Vid. Selsk.* **2**, 4 (1963).
[34] K. Hayashi, T. Shirafuji, *Phys. Rev. D* **19**, 3524 (1979).
[35] J. B. Jimenez, L. Heisenberg and T. Koivisto, *Phys. Rev. D* **98**, 044048 (2018).
[36] J. B. Jimenez et al., *Phys. Rev. D* **101**, 10 (2020).
[37] R. Lazkoz, F.S.N. Lobo, M. Ortiz-Bano, V. Salzano, *Phys. Rev. D* **100**, 104027 (2019).
[38] N. Frusciante, *Phys. Rev. D* **103**, 4 (2021).
[39] M. Koussour et al., *Phys. Dark universe* **36**, 101051 (2022).
[40] M. Koussour and M. Bennai *Chin. J. Phys.* **379**, 339-347 (2022).
[41] M. Koussour et al. *Phys. Ann. Phys.* **445**, 169092 (2022).
[42] M. Koussour and A. De, *Eur. Phys. J. C* **83**, 400 (2023).
[43] M. Koussour et al., *Fortschr. Phys.* **71**, 2200172 (2023).
[44] M. Koussour et al., *Nucl. Phys. B* **990**, 116158 (2023).
[45] M. Koussour et al., *J. High Energy Phys.* **37**, 15-24 (2023).
[46] M. Koussour et al., *J. High Energy Astrophys,* **35**, 43-51 (2022).
[47] T. Harko et al., *Phys. Rev. D* **98**, 8 (2018).
[48] Y. Xu et al., *Eur. Phys. J. C* **79,** 708 (2019).
[49] L. Pati, B. Mishra, and S. K. Tripathy, *Phys. Scr.* **96**, 105003 (2021).
[50] A.S. Agrawal et al., *Phys. Dark Univ.* **33**, 100863 (2021).
[51] S. Bhattacharjee, P.K. Sahoo, *Eur. Phys. J. C* **80**, 289 (2020).
[52] S. K. J. Pacif, *Eur. Phys. J. Plus*, **135**, 10 (2020).
[53] S. K. J. Pacif, R. Myrzakulov and S. Myrzakul, *Int. J. Geom. Methods Mod.*, **14**, 07, (2017).
[54] S. Arora et al., *Phys. Dark Univ.* **30**, 100664 (2020).
[55] Tee-How Loo, M. Koussour, and Avik De, *Ann. Phys.* **454**, 169333 (2023).
[56] M. Tayde, Z. Hassan, P. K. Sahoo, *Chinese Phys. C* **46**, 115101 (2022).
[57] M. Chevallier and D. Polarski, *Int. J. Mod. Phys. D* **10**, 213 (2001).
[58] E. V. Linder, *Phys. Rev. Lett.* **90**, 091301 (2003).

[59] H. K. Jassal, J. S. Bagla, T. Padmanabhan, *Mon. Not. R. Astron. Soc. Lett.* **356**, L11-L16 (2005).

[60] J.-Z. Ma and X. Zhang, *Phys. Lett. B* **669**, 233 (2011).

[61] A. Mukherjee and N. Banerjee, *Eur. Phys. J. Plus*, **130**, 10 (2015).

[62] Y. Gong and Y. Zhang, *Phys. Rev. D*, **72**, 043518 (2005).

[63] W. Yang et al., *Phys. Rev. D*, **99**, 043543 (2019).

[64] R. D. Blandford et al., *Observing Dark Energy*, **339**, 27 (2005) arXiv:astro-ph/0408279.

[65] V. Sahni, T. D. Saini, A. A. Starobinsky, U. Alam, *JETP Lett.* **77**, 201 (2003).

[66] A. Raychaudhuri, *Phys. Rev.* **98**, 1123 (1955).

[67] S. Arora and P. K. Sahoo, *Phys. Scr.* **95**, 9 (2020).

[68] M. Visser, C Barcelo, *COSMO-99*, 98 (2000).

[69] D. F. Mackey et al., *Publ. Astron. Soc. Pac.* **125**, 306 (2013).

[70] C. Blake et al., *Mon. Not. Roy. Astron. Soc.* **418**, 1707 (2011).

[71] W. J. Percival et al., *Mon. Not. Roy. Astron. Soc.* **401**, 2148 (2010).

[72] F. Beutler et al., *Mon. Not. Roy. Astron. Soc.* **416**, 3017 (2011).

[73] N. Jarosik et al., *Astrophys. J. Suppl.* **192**, 14 (2011).

[74] D. J. Eisenstein et al., *Astrophys. J.* **633**, 560 (2005).

[75] R. Giostri et al., *J. Cosm. Astropart. Phys.* **1203**, 027 (2012).

[76] G.S. Sharov, V.O. Vasilie, *Mathematical Modelling and Geometry* **6**, 1 (2018).

[77] D.M. Scolnic et al., *ApJ* **859**, 101(2018).

[78] J. Roman-Garza et al.,*Eur. Phys. J. C* **79**, 890 (2019).

[79] J.F. Jesus et al.,*J. Cosmol. Astropart. Phys.* **04**, 053 (2020).

[80] A. Hernandez-Almada et al.,*Eur. Phys. J. C* **79**, 12 (2019).

[81] S. Basilakos, F. Bauer, and J. Sola,*J. Cosmol. Astropart. Phys.* **01**, 050 (2012).

[82] C. Gruber and O. Luongo, *Phys. Rev. D* **89**, 103506 (2014).

[83] S. Arora, A. Parida and P.K. Sahoo , *Eur. Phys. J. C* **81**, 1-7 (2021).

[84] N. Myrzakulov et al., *Eur. Phys. J. Plus* **138**, 852 (2023).